Zn-Matrix Syntactic Foams: Effect of Heat Treatment on Microstructure and Compressive Properties

Liwen Pan, Yi Yang, Muhammad Usman Ahsan, Dung Dinh Luong, Nikhil Gupta, Ajay Kumar, Pradeep K. Rohatgi

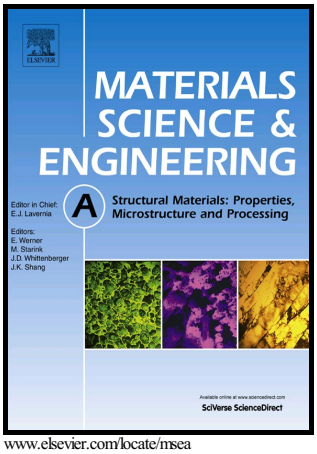

www.elsevier.com/locate/msea

PII: S0921-5093(18)30867-0
DOI: https://doi.org/10.1016/j.msea.2018.06.072
Reference: MSA36627

To appear in: *Materials Science & Engineering A*

Received date: 1 June 2018
Revised date: 15 June 2018
Accepted date: 18 June 2018

Cite this article as: Liwen Pan, Yi Yang, Muhammad Usman Ahsan, Dung Dinh Luong, Nikhil Gupta, Ajay Kumar and Pradeep K. Rohatgi, Zn-Matrix Syntactic Foams: Effect of Heat Treatment on Microstructure and Compressive Properties, *Materials Science & Engineering A,* https://doi.org/10.1016/j.msea.2018.06.072

Zn-Matrix Syntactic Foams: Effect of Heat Treatment on Microstructure and Compressive Properties

Liwen Pan[a,b], Yi Yang[a], Muhammad Usman Ahsan[a], Dung Dinh Luong[a], Nikhil Gupta[a*], Ajay Kumar[c], Pradeep K. Rohatgi[c]

[a]Composite Materials and Mechanics Laboratory, Department of Mechanical and Aerospace Engineering, Tandon School of Engineering, New York University, Brooklyn, NY 11201, USA

[b]School of Resources, Environment and Materials, Guangxi University, Nanning, 530004, China

[c]Materials Department, University of Wisconsin, Milwaukee, WI 53201 USA

[*]Corresponding author. Tel.: +1-646-997-3080. ngupta@nyu.edu.

Abstract

Glass microballoon filled ZA8 alloy matrix syntactic foams are studied for the effect of heat treatment on the microstructure, compressive properties and energy absorption capacity. Normalizing and quenching resulted in reduction or dissolution of eutectic (α+η) phase in the matrix alloy. Blocky Al_3Ni precipitates were observed in the matrix due to the reaction between matrix and the nickel coating of the particles. The average density and porosity of the syntactic

foam were around 3 g/cm^3 and 51.5%, respectively. The heat-treated composites had higher yield strength, compressive strength, plateau stress, densification strain and energy absorption capacity than the as-cast composite. The normalized and quenched composites showed the highest compressive strength, plateau stress and energy absorption capacity. In fact, their highest values were 216.8 MPa and 211.9 MPa, 226.9 MPa and 223.4 MPa, and 125.3 MJ/m^3 and 117.7 MJ/m^3, respectively. The improvement in the compressive properties is attributed to composition homogenization of alloying elements and relief of the residual stresses. The superior properties of syntactic foams compared to those of the conventional metal foams suggest their potential applications in marine vessels and submarine structures.

Keywords: ZA8 alloy; Zinc alloy; syntactic foam; heat treatment; compressive property; energy absorption.

1 INTRODUCTION

Zinc alloys have found numerous applications due to their castability, ease of machining and corrosion resistance [1-3]. Nearly half of the world's consumption of zinc is in the form of coatings, especially for corrosion protection of steel. However, high density (~7.1 g/cm^3) and low melting temperature of Zn-alloys are limitations in many potential applications, which can benefit from development of lightweight zinc matrix composites, particularly syntactic foams. Metal matrix syntactic foams (MMSFs) are synthesized by dispersing hollow particles in a

metallic matrix [4-6]. The presence of porosity in the form of hollow particles provides these materials with closed-cell structure and makes them lightweight compared to the matrix alloy. Available studies on a variety of MMSFs have shown that these composite foams can possess high energy absorption, damping of sound and vibration, heat insulation, and specific stiffness [7, 8]. Many existing applications of zinc alloys in automobiles and marine vessels can benefit from development of lightweight syntactic foams [9].

Aluminum [10-14], steel [15, 16], titanium [17, 18] and magnesium [19-22] matrix syntactic foams have been studied in recent years, which show great potential for the concept of incorporating hollow particles for obtaining lightweight composites with desired properties. These studies have shown that syntactic foams have higher strength and modulus than gas porosity foams at the same density levels. Open-cell and closed-cell zinc foams have also been studied. Heydari et al. [23] synthesized ZA22 alloy closed-cell foams by means of melt foaming using a hydride foaming agent. The resulting foam was found to have high compressive strength but fractured in brittle mode. Sánchez-Martínez et al. [24] used NaCl particles as space holders to fabricate Zn-22Al-2Cu open-cell foams by means of centrifugal infiltration casting process. After solidifications, the NaCl particles were completely dissolved in water using ultrasonic vibrations. These open-cell Zn-22Al-2Cu foams showed increased compressive properties with decreasing pore size. Liu et al. [25] fabricated Zn-Al matrix composite foams reinforced with Al_2O_3 short fibers by means of melt foaming process. The microstructure of the foam was found to

have a significant effect on the compressive behavior and the composite foam exhibited improved energy absorption characteristics.

Liu et al. [26, 27] used $CaCO_3$ as blowing agent to fabricate closed-cell ZA22 foams by melt foaming method. The study shows that the compressive strength and energy absorption capacity of foams under dynamic loading are much greater than those under quasi-static loading condition for certain relative density, which demonstrates remarkable strain rate sensitivity. The plastic collapse stress of ZA22 foams increases with increasing relative density. The relationship between relative plastic collapse stress and relative density was found to follow the Gibson-Ashby model.

Liu et al. [28] used SiC particles as reinforcement and stabilizing agent, and $CaCO_3$ as blowing agent to fabricate ZA22/SiC_p composite foams. The results show that the presence of the SiC_p makes the composite foams more brittle and causes larger stress fluctuation than Zn-22Al alloy foams under compressive loading. However, the composite foams exhibit slightly high energy absorption capacity, although low energy absorption efficiency, as compared with ZA22 foams. Liu et al [29] prepared Al_2O_3 short fiber reinforced closed-cell ZA22 composite foams by means of melt foaming method using $CaCO_3$ as blowing agent. The experimental results indicated that ZA22/Al_2O_3 composite foams show better compressive properties than ZA22 foams. The compressive curves of the composite foams exhibited a smooth plateau region. Kitazono [30] used the powder metallurgical process to prepare closed-cell Zn-22Al eutectoid alloy foams. The heat treated ZA22 foams show ductile compressive deformation at room temperature. The strain

rate sensitivity exponent and absorbed energy were much higher than those of the conventional aluminum foams.

Research on Zn-based syntactic foams is scarce [31]. A study used stir casting method to synthesize ZA22 alloy matrix syntactic foams with varying volume fraction of Ni-coated fly ash cenospheres [31]. The results showed that the foam displayed superior compressive properties and energy absorption capacity compared to those of the conventional foams, suggesting their potential use in engineering structures.

Melt infiltration methods are promising for synthesizing metallic syntactic foams due to their relatively low cost and near net-shape forming of parts [5, 32, 33]. Such methods are capable of producing syntactic foams with high volume fraction of particles because a packed bed is first created to infiltrate with molten metal. In the present work, the pressure infiltration method is used so that lightweight syntactic foams with a high particle content can be synthesized. The syntactic foams are subjected to various heat treatment conditions and then investigated for microstructure and compressive behavior and energy absorption capacity.

2 EXPERIMENTAL PROCEDURES

2.1 Pressure infiltration casting process

ZA8 zinc alloy from Rotometals with nominal composition of 8-9 wt.% Al, 1 wt.% Cu, and 90-91 wt.% Zn was used as the matrix. K46 glass microballoons (GMBs) supplied by 3M were used as reinforcement. These GMBs have nominal true particle density of 460 kg/m^3 and

diameter of 40 μm. GMBs were coated with Ni using a sputter coating method to promote interfacial bonding with the matrix alloy. Borosilicate glass tubes of 15 mm diameter were used as mold for synthesizing syntactic foams. The glass tubes were coated with super enhanced graphite to avoid possible reactions at the tube surface. The tubes were tap-packed with Ni coated GMBs to a height of 25 mm. A 2-mm-thick layer of zirconia felt was placed on top of the GMB bed and an ingot of ZA8 alloy was placed on top of the felt layer as illustrated in Fig. 1. The zirconia felt acts as a filter to remove the oxide layer from the molten metal and a barrier to avoid any reaction between the molten matrix and the reinforcement before infiltration. The assembly was heated in a furnace under vacuum to 525 °C and held at this temperature for 60 minutes, at which time the alloy had fully melted and created a uniform seal on the inner perimeter of the borosilicate glass tube (Fig. 1a). Then, the chamber of the furnace was pressurized to 1 MPa by argon gas and held for 5 minutes (Fig. 1b). The pressure difference between the particle bed and outside of the tube causes infiltration. The remaining ZA8 melt above and the syntactic foam below the zirconia felt were furnace cooled together. The solidified alloy portion was also tested to obtain the baseline alloy properties.

2.2 Heat treatment process

The existing data about heat treatment of ZA8 alloy is scarce so a variety of treatments were designed in this study as described in Table 1 [34]. The heating temperatures were set under

365°C because ZA8 alloy melts between 375~390°C. The heat treatment experiments were performed in a Thermo Scientific Thermolyne Furnace (Model type: F6000).

2.3 Microstructure and phase analysis

Specimens for microstructural observations were prepared using standard metallographic procedures, including grinding, polishing, and etching. The as-cast specimens were freeze fractured and sputter coated with gold before scanning electron microscopy. A Hitachi S-3400N scanning electron microscope (SEM) was used to observe microstructures of ZA8 syntactic foam and the matrix alloy. An energy dispersive spectroscope (EDS) was used to detect the phase compositions and elements.

2.4 Quasi-static compression testing

Specimens of nominal dimensions 7 mm diameter and 3.5 mm thickness were machined from the cast pieces and were tested using an Instron 4467 universal testing frame. Crosshead velocity was maintained constant during the test as per initial strain rate of 2.6×10^{-3} s^{-1}. Load and displacement data recorded during the experiment were used to generate the engineering stress-strain curves from which the material properties are calculated.

3 RESULTS AND DISCUSSION

3.1 As-cast microstructure

Fig. 2 shows microstructure of the as-cast ZA8 alloy and syntactic foams. Well-developed primary Zn-rich dendrites surrounded by the lamellar eutectic structure are observed in the alloy in Fig. 2(a). It has been reported that the eutectic transformation occurs at 382 °C with α-aluminum rich face centered cubic phase and η-Zn rich hexagonal close packed phase [35, 36]. Fig. 2b shows microstructure of the polished syntactic foam (the bright filling inside some GMBs is polishing debris). GMBs are distributed uniformly in the matrix and retained their sphericity despite a rigorous synthesis process. In the ZA8 matrix, the primary Zn-rich phase and discontinuous lamellar (α+η) eutectic mixture were observed. In the higher magnification image Fig. 2(c), dark blocky phases distributed in the matrix are observed. Compared to these images of polished specimens, Fig. 2(d) shows freeze fractured surface of a syntactic foam, where only a few crushed GMBs are observed but most of the GMBs are intact. GMBs crushed during synthesis can be identified because they are usually filled with matrix alloy. GMBs with defects or thin walls are among those that break during synthesis.

Fig. 3 shows the locations where EDS analysis is conducted to determine the composition of various phases in the syntactic foam microstructure. According to the results presented in Table 2, the atomic ratio of Al and Ni in the dark blocky phases is about 3:1, corresponding to Al_3Ni intermetallic phase. The nickel surface coating of GMBs dissolves during syntactic foam synthesis, leading to formation of these intermetallic precipitates. The formation of Al_3Ni phase

has been reported in aluminum matrix composites below the Al-Al_3Ni eutectic temperature of 640^oC [37, 38] and this appears before the zinc-aluminum liquidus phase starts solidifying. The formation of Al_3Ni phase consumes aluminum from the liquidus phase, which reduces the volume of eutectic lamellar structure and increases the primary zinc-rich phase in the microstructure. Therefore, the matrix microstructure in syntactic foams resembles that of zinc alloys with low aluminum content, such as ZA3 alloy [39]. EDS results on the GMB surface shown in Fig. 4 provide evidence of dissolving the Ni layer from GMBs surface.

3.2 Microstructure of heat treated specimens

Microstructures of syntactic foams subjected to various heat treatments listed in Table 1 are presented in Fig. 5. Annealing (furnace cooling) results in coarser (α+η) eutectic mixture in Fig. 5a compared to the as-cast syntactic foam (Fig. 2c). In comparison, the normalized microstructures shown Fig. 5b and Fig. 5c and the quenched microstructure shown in Fig. 5d have little eutectic mixture in the matrix. The solution-aged microstructures presented in Fig. 5e-g, show fine (α+η) eutectic precipitates distributed in the matrix. In addition, some dark, blocky precipitates also appear in the matrix close to GMBs in all heat treated syntactic foams, which is confirmed to be Al_3Ni by EDS results presented in Fig. 6. These precipitates show some deviation from the ideal composition due to the dissolved Zn and Cu elements. Al_3Ni intermetallic is a common phase seen in Al-Ni alloys [38, 40, 41] and it is known to provide high temperature strengthening. Little change can be found in the morphology of Al_3Ni phase after

heat treatment, which is attributed to the long term thermal stability of this phase under 508℃ [42]. These observations show that the cooling rate is one of the primary factors affecting the microstructure in these materials. The lower cooling rate in annealing produces coarse (α+η) eutectic structure, while higher cooling rates of normalizing and quenching produce suppress precipitation of eutectic mixture. The fast cooling rate of quenching combined with low aging temperature can provide the desired combination of grain size and eutectic structure.

3.3 Density and porosity content

The matrix porosity is calculated as 53.2 vol.% using the measured matrix alloy density of 7.2 g/cm^3 in rule of mixtures. In addition, a Skyscan 1172 micro-CT scanner was used to compute the volume porosity of the as-cast syntactic foams as 52.9%, which deviates by only 0.3% from the density based calculations and validates the result. The volume fraction of GMBs (V_f) in the specimens was theoretically calculated by [43]:

$$P_{th} = V_f \left(1 - \frac{t}{R}\right)^3 \quad (2)$$

where P_{th} is porosity in syntactic foams, and t and R represent GMB wall thickness and radius, respectively. The wall thickness of GMBs is estimated to be 1.1 μm using true particle density and particle diameter. It can be observed in Table 3 that there is a very small difference among densities of the syntactic foams, indicating a homogeneous distribution of GMBs across various specimens. The average density of the syntactic foam is 3 g/cm^3, 51.6% lower than that of ZA8 alloy. This density is also lower than those Zn-based syntactic foams reported by Daoud [31], as

shown in Table 4 [4, 15, 24, 27, 28, 30, 31, 44-49]. Although porosity in syntactic foams cannot reach to the level of some metal foams (70-95%), the comparison shows the range of densities that can be obtained in various foams and these values can be used for calculating specific properties.

3.4 Compressive behavior

3.4.1 Compressive deformation behavior

Fig. 7 presents the engineering stress-strain curves for syntactic foams tested under quasi-static compression. The ZA8 alloy shows an elastic limit of about 200 MPa, followed by strain hardening. Stress-strain curve of ZA8 syntactic foams exhibit three distinct regions: an initial linear-elastic response up to the peak strength (I), followed by a long stress plateau (II), and the final densification stage that starts at 50-60% strain (III). These features are similar to those of other metal foams [4, 9, 49-52]. Generally, the transition from I to II has a distinct peek due to progressive collapse of GMBs in a small region after the fracture of the first one and the stress at this peek is taken as the compressive strength. The strain hardening behavior seen in the matrix alloy is not observed in syntactic foams, making them more suitable for energy absorption and damping applications. The strain hardening in matrix is balanced by the volume compaction due to collapse of GMBs to result in the stress plateau in the engineering stress-strain curves.

3.4.2 Compressive properties

Compressive properties of syntactic foams are presented in Table 5. It can be noted that the yield strength (σ_y=$\sigma_{0.2\%}$) of syntactic foams is lower than that of the matrix alloy (229.7 MPa). Heat treatments have helped in improving the yield strength compared to that of the as cast syntactic foams. Compressive strength and plateau stress σ_{pl} (average stress between the strain corresponding to the initial peak (ε_p) and the densification strain (ε_d) [53]) are also found to improve by heat treatments. Fig. 7 shows the tangent method used to calculate ε_d [25, 51]. Among the heat treatments, 360°C/2h/AC normalizing and 365°C/2.5h/WQ quenching processes are found to be particularly effective in improving the yield strength, compressive strength and plateau stress. The highest yield strength, compressive strength and plateau stress appear at 360°C/2h/AC normalizing, which reach up to 176.4, 216.8 and 226.9 MPa, respectively. The highest yield strength shows more than 100% increase over the as-cast syntactic foam. Moreover, Table 5 shows the densification strain (ε_d) has improved after heat treatment, with 365°C/2.5h/AC normalizing process achieving over 18% improvement compared to the as-cast syntactic foams. The comparison of the compressive strength and plateau stress from the present work with several conventional metal foams is presented in Table 6 [9, 23, 24, 44, 46, 49, 53-56]. The compressive properties of syntactic foams are higher than those of most of the foams listed in Table 6, indicating that the Zn matrix syntactic foams can find structural applications.

The higher yield strength, compressive strength and plateau stress of the normalized and quenched specimens are attributed to finer (α+η) eutectic structure (Fig. 5a) obtained under heat

treatment conditions compared to annealed and solution-aged specimens. In addition, presence of high temperature stabile Al_3Ni phase, even in small amounts, also contributes to strengthening, especially because of its fine particle size (<10 μm), similar to previous studies reported on aluminum alloys [38, 41, 57]. This phase is also expected to improve the high temperature stability of syntactic foams. There are other possible reasons contributing to the improved compressive properties of heat treated syntactic foams, which are not fully explored in the study but are likely to affect the results. First, the contrast among phases in micrographs reduces in all heat treated syntactic foams compared to the as-cast syntactic foams, which is likely due to composition homogenization. Second, residual stresses due to difference in thermal expansion coefficient of matrix and GMB materials may decrease in heat treated specimens compared to the as cast specimens. These residual stresses achieve different degrees of relief after different heat treatments and improve the compressive properties to different levels. Third, as seen from Table 3, densities of all the heat treated specimens are higher than the as-cast specimens. Improvement in mechanical properties due to densification after heat treatment has been reported previously [58, 59] and is likely to be a factor in the measured mechanical properties in the present study.

3.4.3 Energy absorption

The energy absorption capacity (W) is determined by calculating the area under the compressive stress-strain curve up to the densification strain (ε_d) by [60]:

$$W = \int_0^{\varepsilon_d} \sigma(\varepsilon) d\varepsilon \quad (3)$$

where W has units corresponding to the energy per unit volume of the material (MJ/m^3). The energy absorption capacity of Zn matrix syntactic foams is given in Table 7, and the energy absorption capacities at different strains are plotted as Fig. 8. It can be observed that there is no abrupt transition in the curves at any strain value corresponding to elastic or plateau regions. Syntactic foams can be divided into three categories based on the energy absorption capacity: (a) normalized and quenched with W in the range of 117~125 MJ/m^3 (b) annealed and solution-aged with W in the range of 102~107 MJ/m^3 and (c) the as-cast with W of 75.8 MJ/m^3. This trend of values with respect to various heat treatments is similar to that observed in the compressive strength and plateau stress values in Table 5. The comparison of energy absorption capacity between the present work and metal matrix syntactic foams reported in the published literature is presented in Table 8 [4, 9, 11, 15, 28, 31, 46, 47, 49, 50, 53, 54, 56, 61-66]. The superior energy absorption capacity of the present syntactic foams is well above most other foams, indicating that the Zn syntactic foams can be used in energy absorption applications.

The energy absorption efficiency is defined as the ratio of the energy absorbed by a material to the energy absorbed by an ideal energy absorber at a given strain and is calculated by [31, 67]:

$$\xi = \frac{A_{real}}{A_{ideal}} = \frac{\int_0^{\varepsilon_d} \sigma(\varepsilon) d\varepsilon}{\sigma_{max}\ \varepsilon_d} \quad (4)$$

where σ_{max} is the highest compressive stress up to ε_d. In addition, the specific energy absorption (E_s) is used to describe the crashworthiness of a material. It can evaluate the magnitude of absorbed energy at the same mass and is defined by [4]:

$$E_s = \frac{W_{\varepsilon_d}}{\rho_{sf}} \tag{5}$$

where W_{ε_d} is energy absorption capacity of the material, and ρ_{sf} is density. The ξ and E_s of syntactic foams heat treated under different conditions are given in Table 7. It is observed that the higher compressive strength and plateau stress correspond to higher energy absorption efficiency and specific energy absorption efficiency. The group with highest ξ and E_s is the one that is normalized and quenched, followed by annealed and solution-aged specimens, while the values for the as-cast specimens are the lowest. The highest E_s is noted for 365°C/2.5h/AC normalized syntactic foam, 41.8 kJ/kg, which far surpasses the conventional metal foams and is also higher than the values reported for most metal matrix syntactic foams in Table 8. This observation indicates that the heat treatment can simultaneously improve the compressive properties and energy absorption efficiency and can be beneficial for applications.

CONCLUSIONS

The microstructure, compressive properties and energy absorption capability of a ZA8-matrix syntactic foams filled with Ni-coated GMBs are studied with and without heat treatment. The main conclusions are summarized as:

(1) The amount of β-Zn phase and eutectic mixture depend on the cooling rate in the heat treatment process. The high temperature stable Al_3Ni phase is stable in the microstructure in the processing temperature range.

(2) The average density and porosity of the syntactic foam are 3 g/cm^3 and 51.5%, respectively. All the heat treated syntactic foams have higher yield strength, compressive strength, plateau stress and densification strain than the as-cast syntactic foams. The normalized and quenched foams show higher compressive properties than others, and their yield strength, compressive strength, plateau stress reach up to 176.4 and 148.1, 216.8 and 211.9, 226.9 and 223.4 MPa, respectively. Analysis indicates that the improvement in the compressive properties is mainly attributed to composition homogenization, relief of the residual compressive stress and presence of Al_3Ni phase.

(3) The energy absorption capacity and specific energy absorption of the syntactic foams after normalizing and quenching process are in the range of 117-125 MJ/m^3 and 39.2-41.8 kJ/kg, respectively, and for the annealing and solution-aging process, are in the range of 102-107 MJ/m^3 and 34-36 kJ/kg, respectively. The syntactic foams show superior energy absorption capacity than the conventional metal foams and many metal matrix syntactic foams.

ACKNOWLEDGEMENTS

The authors acknowledge the National Science Foundation US-Egypt Cooperative Research Project (Award # OISE 1445686). Dr. Paulo Coelho is thanked for providing access to EDS for some of the measurements.

DATA AVAILABILITY STATEMENT

The raw/processed data required to reproduce these findings cannot be shared at this time as the data also forms part of an ongoing study. Interested researchers should send request to the corresponding author for sharing the data with their specific purpose.

REFERENCES

1. Apelian, D., Paliwal, M., and Herrschaft, D.C., *Casting with Zinc Alloys.* JOM, 1981. **33**(11): p. 12-20.
2. Murphy, M., *Zinc and zinc alloys.* Metal Finishing, 1996. **94**(2): p. 26-27.
3. Prasad, B.K., Patwardhan, A.K., and Yegneswaran, A.H., *Microstructure and property characterization of a modified zinc-base alloy and comparison with bearing alloys.* Journal of Materials Engineering and Performance, 1998. **7**(1): p. 130-135.
4. Broxtermann, S., Taherishargh, M., Belova, I.V., Murch, G.E., and Fiedler, T., *On the compressive behaviour of high porosity expanded Perlite-Metal Syntactic Foam (P-MSF).* Journal of Alloys and Compounds, 2017. **691**: p. 690-697.

5. Altenaiji, M., Guan, Z.W., Cantwell, W.J., Zhao, Y., and Schleyer, G.K., *Characterisation of aluminium matrix syntactic foams under drop weight impact.* Materials & Design, 2014. **59**(Supplement C): p. 296-302.

6. Gupta, N. and Rohatgi, P.K., *Metal Matrix Syntactic Foams: Processing, Microstructure, Properties and Applications*. 2015: Destech Publications, PA.

7. Gupta, N. and Rohatgi, P.K., *4.15 Metal Matrix Syntactic Foams*, in *Comprehensive Composite Materials II*. 2018, Elsevier: Oxford. p. 364-385.

8. Fiedler, T., Öchsner, A., Belova, I.V., and Murch, G.E., *Recent Advances in the Prediction of the Thermal Properties of Syntactic Metallic Hollow Sphere Structures.* Advanced Engineering Materials, 2008. **10**(4): p. 361-365.

9. Vogiatzis, C.A., Tsouknidas, A., Kountouras, D.T., and Skolianos, S., *Aluminum–ceramic cenospheres syntactic foams produced by powder metallurgy route.* Materials & Design, 2015. **85**(Supplement C): p. 444-454.

10. Lamanna, E., Gupta, N., Cappa, P., Strbik, O.M., and Cho, K., *Evaluation of the dynamic properties of an aluminum syntactic foam core sandwich.* Journal of Alloys and Compounds, 2017. **695**(Supplement C): p. 2987-2994.

11. Zhang, Q., Lin, Y., Chi, H., Chang, J., and Wu, G., *Quasi-static and dynamic compression behavior of glass cenospheres/5A03 syntactic foam and its sandwich structure.* Composite Structures, 2018. **83**: p. 499-509.

12. Lin, Y., Zhang, Q., Ma, X., and Wu, G., *Mechanical behavior of pure Al and Al–Mg syntactic foam composites containing glass cenospheres.* Composites Part A: Applied Science and Manufacturing, 2016. **87**(Supplement C): p. 194-202.

13. Katona, B., Szebényi, G., and Orbulov, I.N., *Fatigue properties of ceramic hollow sphere filled aluminium matrix syntactic foams.* Materials Science and Engineering: A, 2017. **679**(Supplement C): p. 350-357.

14. Lin, Y., Zhang, Q., and Wu, G., *Interfacial microstructure and compressive properties of Al–Mg syntactic foam reinforced with glass cenospheres.* Journal of Alloys and Compounds, 2016. **655**(Supplement C): p. 301-308.

15. Castro, G. and Nutt, S.R., *Synthesis of syntactic steel foam using gravity-fed infiltration.* Materials Science and Engineering: A, 2012. **553**(Supplement C): p. 89-95.

16. Peroni, L., Scapin, M., Fichera, C., Lehmhus, D., Weise, J., Baumeister, J., and Avalle, M., *Investigation of the mechanical behaviour of AISI 316L stainless steel syntactic foams at different strain-rates.* Composites Part B: Engineering, 2014. **66**(Supplement C): p. 430-442.

17. Mondal, D.P., Datta Majumder, J., Jha, N., Badkul, A., Das, S., Patel, A., and Gupta, G., *Titanium-cenosphere syntactic foam made through powder metallurgy route.* Materials & Design, 2012. **34**(Supplement C): p. 82-89.

18. Xue, X. and Zhao, Y., *Ti matrix syntactic foam fabricated by powder metallurgy: Particle breakage and elastic modulus.* JOM, 2011. **63**(2): p. 43-47.

19. Daoud, A., Abou El-khair, M.T., Abdel-Aziz, M., and Rohatgi, P., *Fabrication, microstructure and compressive behavior of ZC63 Mg–microballoon foam composites.* Composites Science and Technology, 2007. **67**(9): p. 1842-1853.

20. Anbuchezhiyan, G., Mohan, B., Sathianarayanan, D., and Muthuramalingam, T., *Synthesis and characterization of hollow glass microspheres reinforced magnesium alloy matrix syntactic foam.* Journal of Alloys and Compounds, 2017. **719**(Supplement C): p. 125-132.

21. Braszczyńska-Malik, K.N. and Kamieniak, J., *AZ91 magnesium matrix foam composites with fly ash cenospheres fabricated by negative pressure infiltration technique.* Materials Characterization, 2017. **128**(Supplement C): p. 209-216.

22. Anantharaman, H., Shunmugasamy, V.C., Strbik, O.M., Gupta, N., and Cho, K., *Dynamic properties of silicon carbide hollow particle filled magnesium alloy (AZ91D) matrix syntactic foams.* International Journal of Impact Engineering, 2015. **82**(Supplement C): p. 14-24.

23. Heydari Astaraie, A., Shahverdi, H.R., and Elahi, S.H., *Compressive behavior of Zn–22Al closed-cell foams under uniaxial quasi-static loading.* Transactions of Nonferrous Metals Society of China, 2015. **25**(1): p. 162-169.

24. Sánchez-Martínez, A., Cruz, A., González-Nava, M., and Suárez, M.A., *Main process parameters for manufacturing open-cell Zn-22Al-2Cu foams by the centrifugal infiltration route and mechanical properties.* Materials & Design, 2016. **108**(Supplement C): p. 494-500.

25. Liu, J.A., Yu, S.R., Hu, Z.Q., Liu, Y.H., and Zhu, X.Y., *Deformation and energy absorption characteristic of Al_2O_{3f}/Zn–Al composite foams during compression.* Journal of Alloys and Compounds, 2010. **506**(2): p. 620-625.

26. Liu, J., Yu, S., Song, Y., Zhu, X., Wei, M., Luo, Y., and Liu, Y., *Dynamic compressive strength of Zn–22Al foams.* Journal of Alloys and Compounds, 2009. **476**(1): p. 466-469.

27. Liu, J., Yu, S., Zhu, X., Wei, M., Luo, Y., and Liu, Y., *The compressive properties of closed-cell Zn-22Al foams.* Materials Letters, 2008. **62**(4): p. 683-685.

28. Liu, J., Yu, S., Zhu, X., Wei, M., Luo, Y., and Liu, Y., *Correlation between ceramic additions and compressive properties of Zn–22Al matrix composite foams.* Journal of Alloys and Compounds, 2009. **476**(1): p. 220-225.

29. Liu, J., Yu, S., Zhu, X., Wei, M., Li, S., Luo, Y., and Liu, Y., *Effect of Al_2O_3 short fiber on the compressive properties of Zn–22Al foams.* Materials Letters, 2008. **62**(21): p. 3636-3638.

30. Kitazono, K. and Takiguchi, Y., *Strain rate sensitivity and energy absorption of Zn–22Al foams.* Scripta Materialia, 2006. **55**(6): p. 501-504.

31. Daoud, A., *Synthesis and characterization of novel ZnAl22 syntactic foam composites via casting.* Materials Science and Engineering: A, 2008. **488**(1-2): p. 281-295.

32. Szlancsik, A., Katona, B., Bobor, K., Májlinger, K., and Orbulov, I.N., *Compressive behaviour of aluminium matrix syntactic foams reinforced by iron hollow spheres.* Materials & Design, 2015. **83**(Supplement C): p. 230-237.

33. Myers, K., Katona, B., Cortes, P., and Orbulov, I.N., *Quasi-static and high strain rate response of aluminum matrix syntactic foams under compression.* Composites Part A: Applied Science and Manufacturing, 2015. **79**(Supplement C): p. 82-91.

34. Chandler, H., *Heat Treater's Guide: Practices and Procedures for Nonferrous Alloys*. 1996, United States: ASM International.

35. Türk, A., Durman, M., and Kayali, E.S., *The effect of manganese on the microstructure and mechanical properties of zinc–aluminium based ZA-8 alloy.* Journal of Materials Science, 2007. **42**(19): p. 8298-8305.

36. Vander Voort, G.F., *Metallography and microstructures of Zinc and its alloys*, in *ASM Handbook, Volume 09 - Metallography and Microstructures*, G.F. Vander Voort, Editor. 2004, ASM International. p. 933–941.

37. Chen, H. and Alpas, A.T., *Wear of aluminium matrix composites reinforced with nickel-coated carbon fibres.* Wear, 1996. **192**(1): p. 186-198.

38. Peng, G., Tietao, Z., Xiaoqing, X., Zhi, G., and Li, C., *Refinement Mechanism Research of Al3Ni Phase in Ni-7050 Alloy.* Rare Metal Materials and Engineering, 2013. **42**(1): p. 6-13.

39. Prosek, T., Hagström, J., Persson, D., Fuertes, N., Lindberg, F., Chocholatý, O., Taxén, C., Šerák, J., and Thierry, D., *Effect of the microstructure of Zn-Al and Zn-Al-Mg model alloys on corrosion stability.* Corrosion Science, 2016. **110**: p. 71-81.

40. Cho, Y.H., Kim, H.W., Kim, W., Jo, D.A., and Lee, J.M., *The Effect of Ni Additions on the Microstructure and Castability of Low Si Added Al Casting Alloys.* Materials Today: Proceedings, 2015. **2**(10, Part A): p. 4924-4930.

41. Uan, J.Y., Lui, T.S., and Chen, L.H., *Superplasticity-like behavior of Al-Al3Ni eutectic alloy.* Materials Chemistry and Physics, 1996. **43**(3): p. 278-282.

42. Uan, J.Y. and Lui, T.S., *The Relationship between Tensile Properties of Extruded Al-Al3Ni Eutectic Alloy and its Cast Structure Control.* Cast Metals, 1994. **6**(4): p. 210-216.

43. Kiser, M., He, M.Y., and Zok, F.W., *The mechanical response of ceramic microballoon reinforced aluminum matrix composites under compressive loading.* Acta Materialia, 1999. **47**(9): p. 2685-2694.

44. Luong, D.D., Strbik, O.M., Hammond, V.H., Gupta, N., and Cho, K., *Development of high performance lightweight aluminum alloy/SiC hollow sphere syntactic foams and compressive characterization at quasi-static and high strain rates.* Journal of Alloys and Compounds, 2013. **550**(Supplement C): p. 412-422.

45. Mondal, D.P., Das, S., Ramakrishnan, N., and Uday Bhasker, K., *Cenosphere filled aluminum syntactic foam made through stir-casting technique.* Composites Part A: Applied Science and Manufacturing, 2009. **40**(3): p. 279-288.

46. Taherishargh, M., Belova, I.V., Murch, G.E., and Fiedler, T., *Pumice/aluminium syntactic foam.* Materials Science and Engineering: A, 2015. **635**(Supplement C): p. 102-108.

47. Bazzaz Bonabi, S., Kahani Khabushan, J., Kahani, R., and Honarbakhsh Raouf, A., *Fabrication of metallic composite foam using ceramic porous spheres "Light Expanded Clay Aggregate" via casting process.* Materials & Design, 2014. **64**(Supplement C): p. 310-315.

48. Castro, G., Nutt, S.R., and Wenchen, X., *Compression and low-velocity impact behavior of aluminum syntactic foam.* Materials Science and Engineering: A, 2013. **578**(Supplement C): p. 222-229.

49. Tao, X.F., Zhang, L.P., and Zhao, Y.Y., *Al matrix syntactic foam fabricated with bimodal ceramic microspheres.* Materials & Design, 2009. **30**(7): p. 2732-2736.

50. Wu, G.H., Dou, Z.Y., Sun, D.L., Jiang, L.T., Ding, B.S., and He, B.F., *Compression behaviors of cenosphere–pure aluminum syntactic foams.* Scripta Materialia, 2007. **56**(3): p. 221-224.

51. Daoud, A., *Compressive response and energy absorption of foamed A359–Al_2O_3 particle composites.* Journal of Alloys and Compounds, 2009. **486**(1-2): p. 597-605.

52. Weise, J., Baumeister, J., Yezerska, O., Salk, N., and Silva, G.B.D., *Syntactic Iron Foams with Integrated Microglass Bubbles Produced by Means of Metal Powder Injection Moulding.* Advanced Engineering Materials, 2010. **12**(7): p. 604-608.

53. Newsome, D.B., Schultz, B.F., Ferguson, J.B., and Rohatgi, P.K., *Synthesis and Quasi-Static Compressive Properties of Mg-AZ91D-Al(2)O(3) Syntactic Foams.* Materials, 2015. **8**(9): p. 6085-6095.

54. Zhang, B., Lin, Y., Li, S., Zhai, D., and Wu, G., *Quasi-static and high strain rates compressive behavior of aluminum matrix syntactic foams.* Composites Part B: Engineering, 2016. **98**(Supplement C): p. 288-296.

55. Licitra, L., Luong, D.D., Strbik, O.M., and Gupta, N., *Dynamic properties of alumina hollow particle filled aluminum alloy A356 matrix syntactic foams.* Materials & Design, 2015. **66**(Part B): p. 504-515.

56. Rocha Rivero, G.A., Schultz, B.F., Ferguson, J.B., Gupta, N., and Rohatgi, P.K., *Compressive properties of Al-A206/SiC and Mg-AZ91/SiC syntactic foams.* Journal of Materials Research, 2013. **28**(17): p. 2426-2435.

57. Kakitani, R., Reyes, R.V., Garcia, A., Spinelli, J.E., and Cheung, N., *Relationship between spacing of eutectic colonies and tensile properties of transient directionally solidified Al-Ni eutectic alloy.* Journal of Alloys and Compounds, 2018. **733**(Supplement C): p. 59-68.

58. Ohji, T. and Jonghe Lutgard, C., *Presintering Heat Treatment, Densification, and Mechanical Properties of Silicon Carbide.* Journal of the American Ceramic Society, 2005. **77**(6): p. 1685-1687.

59. He, P., Jia, D., Lin, T., Wang, M., and Zhou, Y., *Effects of high-temperature heat treatment on the mechanical properties of unidirectional carbon fiber reinforced geopolymer composites.* Ceramics International, 2010. **36**(4): p. 1447-1453.

60. Zhang, Q., Lin, Y., Chi, H., Chang, J., and Wu, G., *Quasi-static and dynamic compression behavior of glass cenospheres/5A03 syntactic foam and its sandwich structure.* Composite Structures, 2018. **183**(Supplement C): p. 499-509.

61. Birla, S., P. Mondal, D., Das, S., Prasanth, N., K. Jha, A., and Chilla, V., *Compressive Deformation Behavior of Highly Porous AA2014-Cenosphere Closed Cell Hybrid Foam Prepared Using CaH_2 as Foaming Agent: Comparison with Aluminum Foam and Syntactic Foam.* Transactions of the Indian Institute of Metals, 2016. **70**(7): p. 1827–1840.

62. Lin, H., Wang, H.Y., Lu, C., and Dai, L.H., *A metallic glass syntactic foam with enhanced energy absorption performance.* Scripta Materialia, 2016. **119**(Supplement C): p. 47-50.

63. Wright, A. and Kennedy, A., *The Processing and Properties of Syntactic Al Foams Containing Low Cost Expanded Glass Particles.* Advanced Engineering Materials, 2017. **19**(11): p. 1600467.

64. Taherishargh, M., Vesenjak, M., Belova, I.V., Krstulović-Opara, L., Murch, G.E., and Fiedler, T., *In situ manufacturing and mechanical properties of syntactic foam filled tubes.* Materials & Design, 2016. **99**(Supplement C): p. 356-368.

65. Santa Maria, J.A., Schultz, B.F., Ferguson, J.B., Gupta, N., and Rohatgi, P.K., *Effect of hollow sphere size and size distribution on the quasi-static and high strain rate compressive properties of Al-A380–Al_2O_3 syntactic foams.* Journal of Materials Science, 2014. **49**(3): p. 1267-1278.

66. Daoud, A., *Effect of strain rate on compressive properties of novel Zn12Al based composite foams containing hybrid pores.* Materials Science and Engineering: A, 2009. **525**(1): p. 7-17.

67. Taherishargh, M., Linul, E., Broxtermann, S., and Fiedler, T., *The mechanical properties of expanded perlite-aluminium syntactic foam at elevated temperatures.* Journal of Alloys and Compounds, 2018. **737**: p. 590-596.

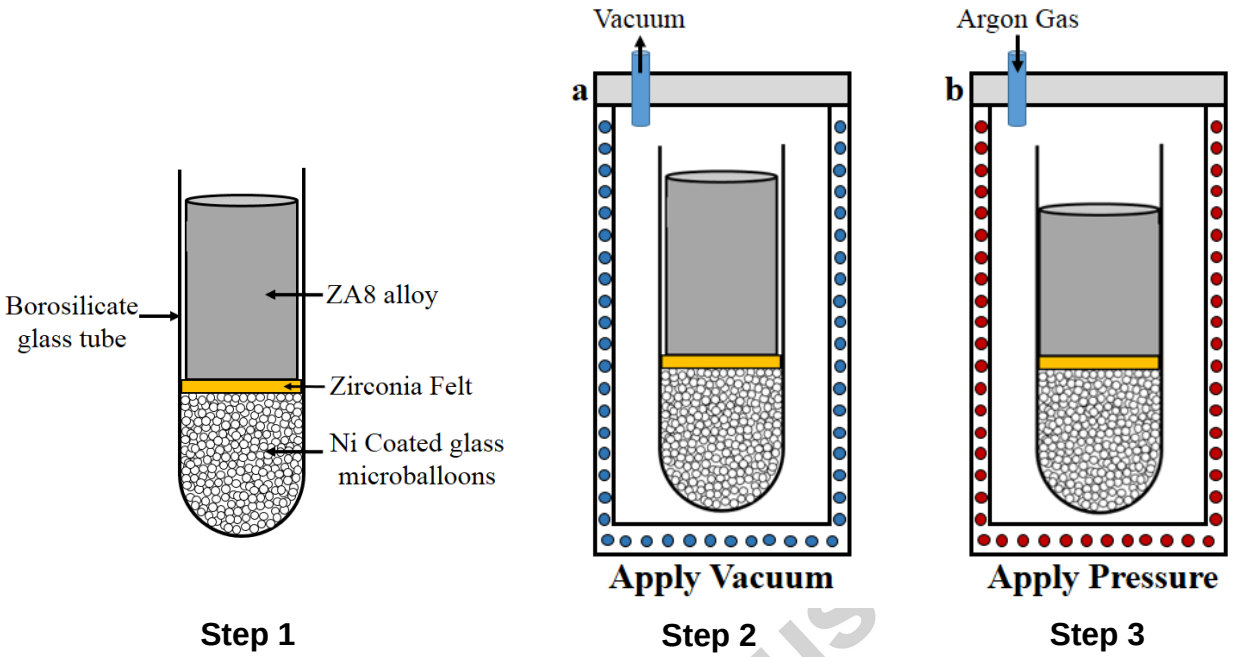

Fig. 1. Schematic representation of the pressure infiltration casting procedure.

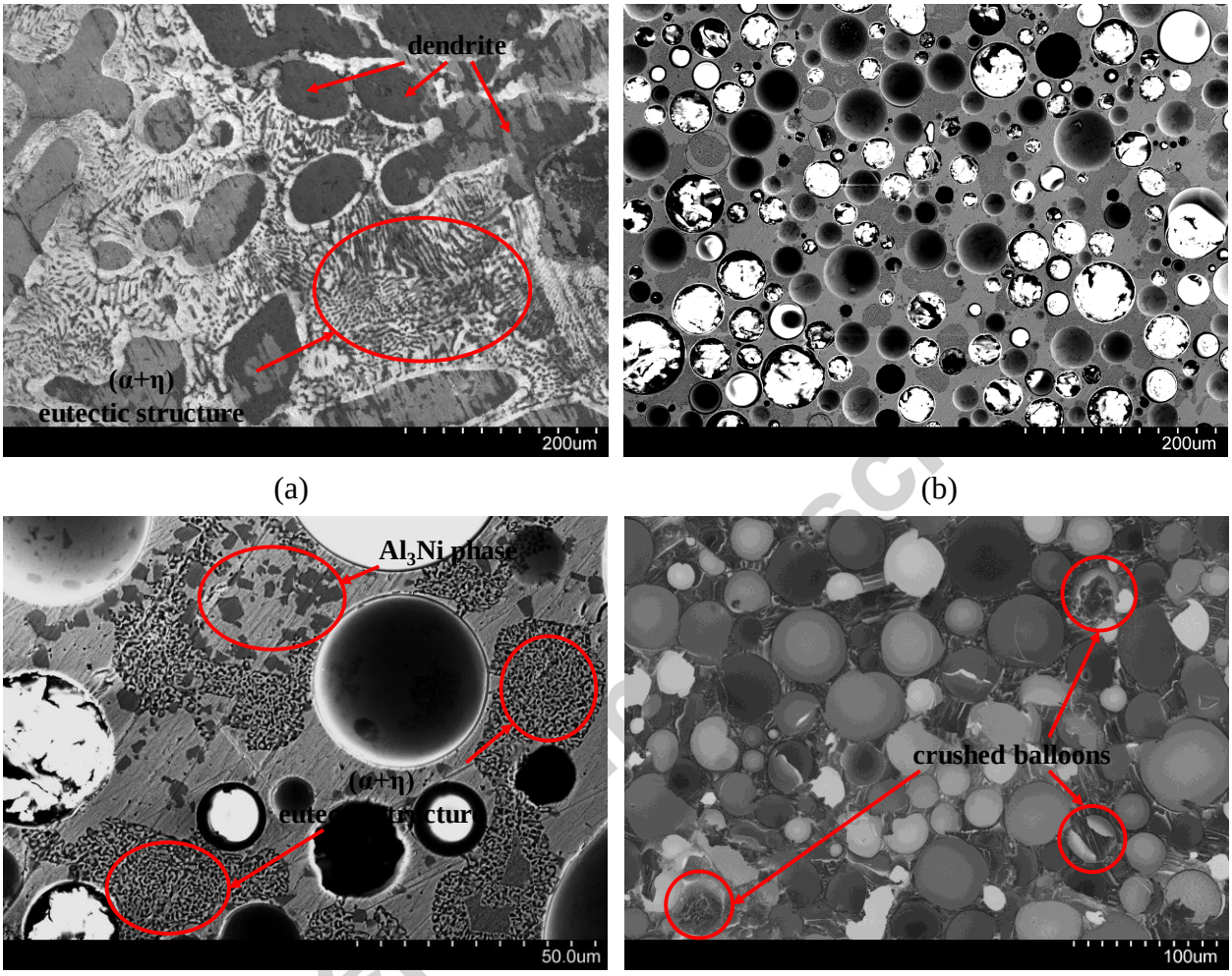

Fig. 2. Micrographs of ZA8 alloy and syntactic foams synthesized by pressure infiltration casting. (a) ZA8 alloy, (b) as-polished ZA8 syntactic foam, (c) as-polished ZA8 syntactic foam at higher magnification and (d) freeze fracture surface of ZA8 syntactic foam.

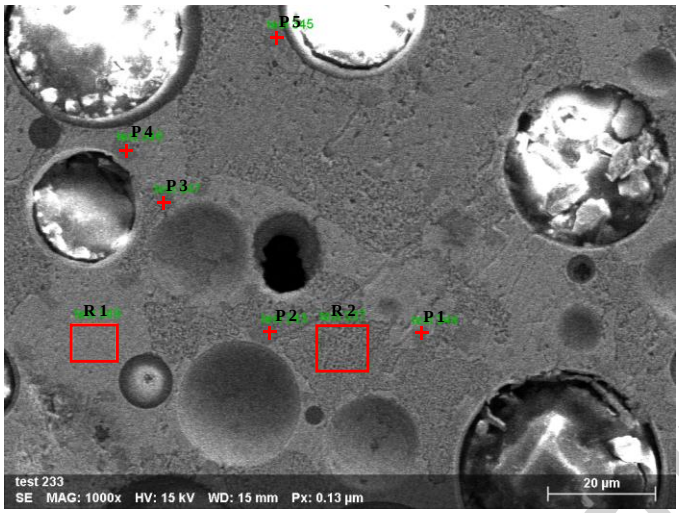

Fig. 3. **Selected regions in the syntactic foam matrix microstructure for EDS analysis.**

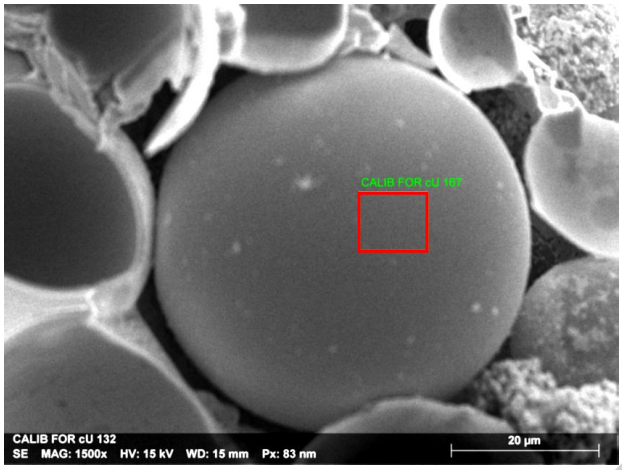

(a)

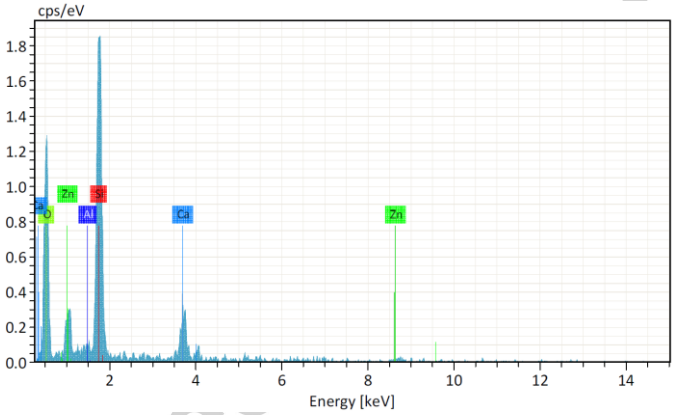

(b)

Fig. 4. EDS analysis of the surface of a GMB: (a) the region of the GMB surface selected for analysis and (b) EDS pattern showing various phases present on the surface.

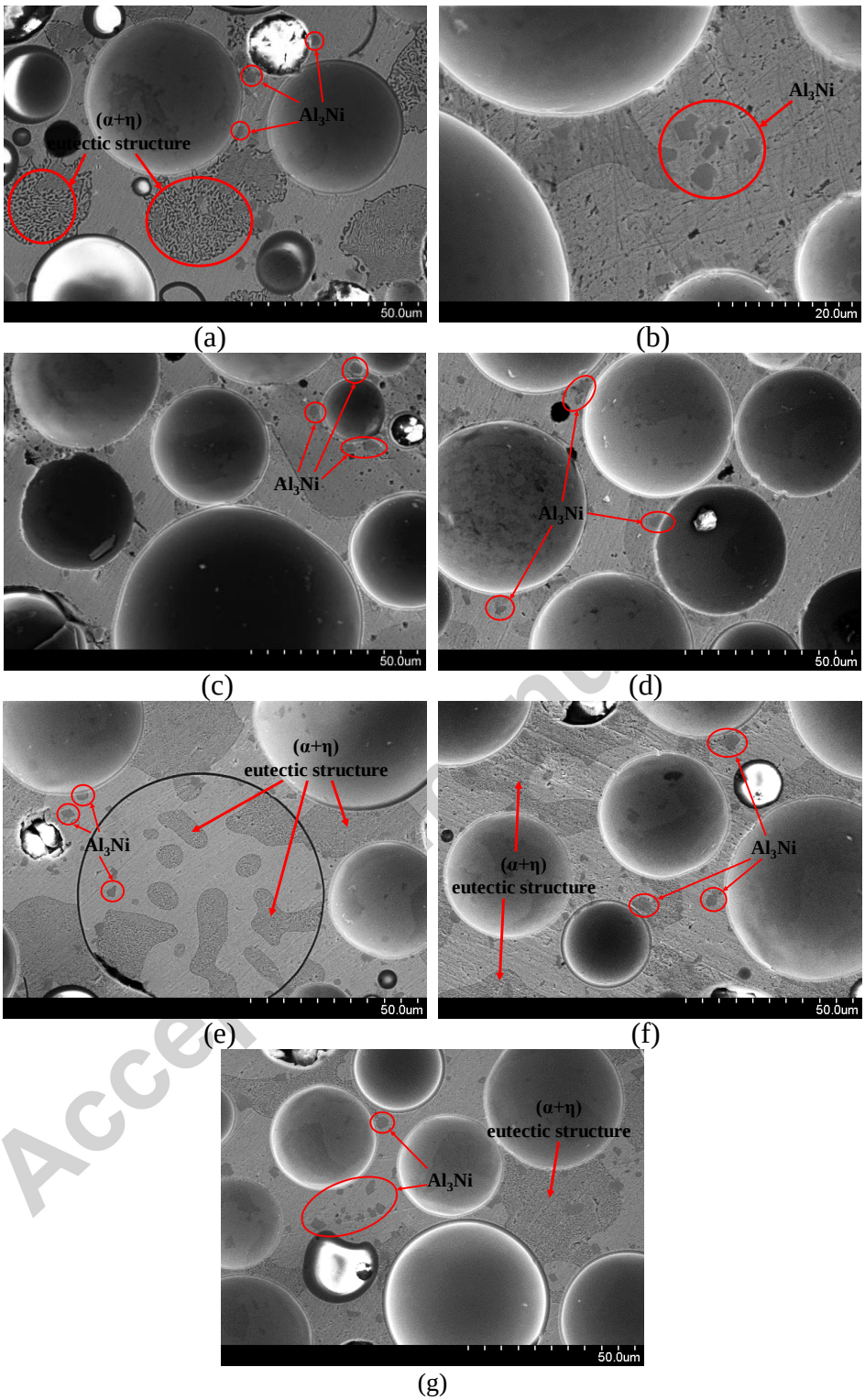

Fig. 5. Microstructure of ZA8 syntactic foam after heat treatment. (a) 365℃/2.5h/FC; (b) 360℃/2h/AC; (c) 365℃/2.5h/AC; (d) 365℃/2.5h/WQ; (e) 365℃/2.5h/WQ+150℃/2h/AC (f) 365℃/5h/WQ+150℃/2h/AC; (g) 365℃/2.5h/WQ+150℃/5h/AC.

(a)

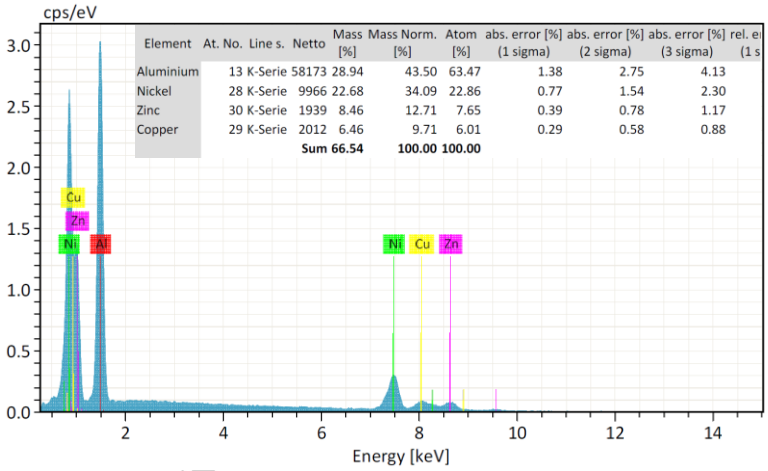

(b)

Fig. 6. EDS analysis of the Al_3Ni phase: (a) location of point spectrum and (b) EDS pattern and composition.

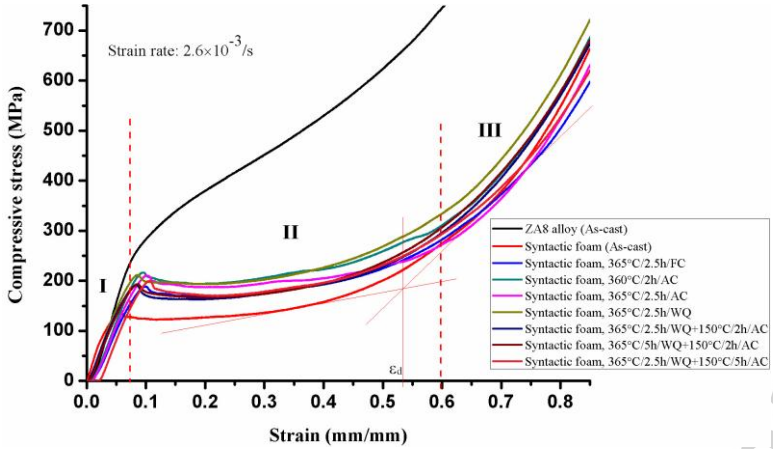

Fig. 7. Stress-strain curves for quasi-static compression tests.

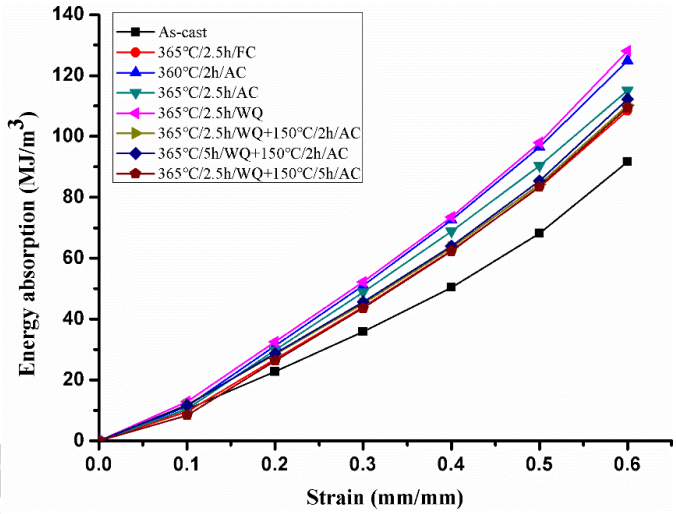

Fig. 8. Energy absorption capacity of syntactic foams at different strains.

Table 1. Heat treatment processes applied to ZA8 syntactic foams.

#	Type of heat treatment	Temp. (°C)	Time (h)	Cooling method	Temp. (°C)	Holding Time (h)	Cooling method
1	Annealing	365	2.5	Furnace cooling	—	—	—
2	Normalizing	360	2	Air cooling	—	—	—
3	Normalizing	365	2.5	Air cooling	—	—	—
4	Quenching	365	2.5	Water quenching	—	—	—
5	Solution-aging	365	2.5	Water quenching	150	2	Air cooling
6	Solution-aging	365	5	Water quenching	150	2	Air cooling
7	Solution-aging	365	2.5	Water quenching	150	5	Air cooling

Table 2. Atomic concentration of various elements in the as-cast syntactic foams (%).

Spectrum number*	Al	Ni	Cu	Zn
R1	3.18	0.00	2.24	94.58
R2	47.51	0.00	0.08	52.41
P1	67.27	28.38	3.39	0.97
P2	63.69	31.28	4.79	0.23
P3	64.12	23.56	6.15	6.16
P4	64.63	22.68	1.77	10.91
P5	65.10	31.68	3.22	0.00

*R represents region and P represents point scan in EDS at locations shown in Fig. 3.

Table 3. Density, porosity and GMB volume fraction in syntactic foams.

Samples condition	Density (g/cm^3)	Porosity (%)	GMB volume fraction (%)
ZA8 matrix alloy (as-cast)	7.2	--	--
Syntactic foam (as-cast)	2.9	53.2/52.9*	63/62.7*
Syntactic foam, 365℃/2.5h/FC	2.92	52.9	62.7
Syntactic foam, 360℃/2h/AC	3.03	51.1	60.6
Syntactic foam, 365℃/2.5h/AC	3.01	51.5	61.0
Syntactic foam, 365℃/2.5h/WQ	3.13	49.5	58.7
Syntactic foam, 365℃/2.5h/WQ+150℃/2h/AC	2.98	51.9	61.5
Syntactic foam, 365℃/5h/WQ+150℃/2h/AC	3.11	49.8	59.0
Syntactic foam, 365℃/2.5h/WQ+150℃/5h/AC	2.96	52.3	62.0
Average value (syntactic foam)	3.00	51.5	61.0

*Measured by micro-CT scan and image analysis.

Table 4. Comparison of porosity in some metal cellular foams and the syntactic foam of the present work.

Foam materials	Process	Porosity (%)	References
ZA8 syntactic foam	Pressure infiltration casting	**53.2**	**Present work**
ZnAl22 syntactic foam	Stir casting	24.5	[31]
ZnAl22 syntactic foam	Stir casting	37.7	[31]
Zn–22Al alloy foam	Powder metallurgy	30-64	[30]
Zn−22Al alloy foam	Melt foaming	59-68	[24]
Zn-22Al foam	Melt foaming	82-94.3	[27]
ZA22/SiCp foam	Stir-casting+melt foaming	81.4-82.3	[28]
A356/SiCHS syntactic foam	Pressure infiltration casting	38	[44]
A2014 Al syntactic foam	Stir-casting	23-38	[45]
A356/pumice syntactic foam	Infiltration casting	~45	[46]
A355.0/ LECA composite foam	Gravity casting	56	[47]
6061 Al syntactic foam	Melt infiltration	54	[48]
Ferritic-pearlitic steel foam	Gravity-fed infiltration	46	[15]
6082 Al syntactic foam	Melt infiltration casting	49-59	[49]
A356 Al/ perlite syntactic foam	Counter gravity infiltration casting	79	[4]

Table 5. Compressive properties of syntactic foams after different heat treatments.

Heat treatment process	Yield strength (MPa)	Compressive strength (MPa)	σ_{pl} (MPa)	ε_d (%)
Syntactic foam (as-cast)	86.8	137.8	148.1	53.6
Annealing, 365℃/2.5h/FC	129.9	188.9	197.4	59.7
Normalizing, 360℃/2h/AC	176.4	216.8	226.9	60
Normalizing, 365℃/2.5h/AC	140	210.9	214.3	63.6
Quenching, 365℃/2.5h/WQ	148.1	211.9	223.4	56.8
Solution-aging, 365℃/2.5h/WQ+150℃/2h/AC	130.6	191.6	192.2	57.8
Solution-aging, 365℃/5h/WQ+150℃/2h/AC	132.8	193.7	194.7	56.8
Solution-aging, 365℃/2.5h/WQ+150℃/5h/AC	135.2	200.2	199.6	58.5

Table 6. Comparison of the compressive properties of syntactic foams of present work with other metal foams.

Foam materials	Yield strength (MPa)	Compressive strength (MPa)	σ_{pl} (MPa)	Reference
ZA8 syntactic foam	87~176	138~217	148~227	**Present work**
6082 Al syntactic foam	53~115	~80-120	44~77	[49]
Al matrix syntactic foam	9~35	36	89.9	[9]
Cp-Al syntactic foam	64.7	75.5	60.8	[54]
A356 Al syntactic foam	48	50~80	76.4	[46]
Zn-22Al foam		2.7~6		[23]
Zn-22Al-2Cu foam	8.6		19.3	[24]
A356 syntactic foam	129.6	143	118.7	[55]
Al-A206 syntactic foam		168.5	121.5	[56]
Mg-AZ91 syntactic foam		118.2	63.7	[56]
A356 syntactic foam		163	110	[44]
Mg-AZ91D Syntactic Foam		168~376	96~205	[53]

Table 7. Energy absorption properties of ZA8 syntactic foam heat treated under different conditions.

Heat treatment process	Densification strain (%)	Energy Absorption capacity (MJ/m^3)	Specific energy absorption (kJ/kg)	Energy absorption efficiency (%)
Matrix alloy (as-cast)	—	—	—	—
Syntactic foam (as-cast)	53.6	75.8	25.3	63.2
Annealing, 365℃/2.5h/FC	59.7	107.7	35.9	64.4
Normalizing, 360℃/2h/AC	60	124.9	41.6	66.9
Normalizing, 365℃/2.5h/AC	63.6	125.3	41.8	66.1
Quenching, 365℃/2.5h/WQ	56.8	117.7	39.2	66.7
Solution-aging, 365℃/2.5h/WQ+150℃/2h/AC	57.8	104	34.7	64.6
Solution-aging, 365℃/5h/WQ+150℃/2h/AC	56.8	102.9	34.3	64.6
Solution-aging, 365℃/2.5h/WQ+150℃/5h/AC	58.5	105.2	35.1	63.7

Table 8. Comparison of compressive energy absorption capacity of syntactic foams of the present work with some metal matrix syntactic foams reported in recent years.

Syntactic foam matrix	Energy absorption capacity (/MJ/m^3)	Specific energy absorption capacity (/kJ/kg)	Reference	Year
ZA8 alloy	125.3	41.8	Present work	2017
5A03 Al alloy	51.2	41.9	[11]	2017
A356 Al alloy	6.6	8.68	[4]	2017
AA2014 alloy	23.5	11.15	[61]	2017
Zr-Ti-Cu-Ni-Be metallic glasses	113.6	35.5	[62]	2016
Al-12Si alloy	7	6.2	[63]	2016
Pure Al	15.42	7	[54]	2016
A356 Al alloy	55.19	23.78	[64]	2016
A356Al alloy	26.5	24.8	[46]	2015
Pure Al	34.88	14.8	[9]	2015
AZ91D Mg alloy	124	53.68	[53]	2015
A380 Al alloy	57.7	31	[65]	2014
A355.0 Al alloy	18	15	[47]	2014
A206 Al alloy	63.2	32.75	[56]	2013
AZ91 Mg alloy	50.7	42.2	[56]	2013
TRIP-steel	104.78	29.2	[15]	2012
6082 Al alloy	30.9	25	[49]	2009
Zn12Al alloy	7	6.7	[66]	2009
Zn-22Al alloy	＜2.5	＜0.9	[28]	2009
ZnAl22 alloy	65.5	19.85	[31]	2008
Pure Al	20~35	14~23	[50]	2007